

Witch Hazel (*Hamamelis virginiana*) Fractions and the Importance of Gallate Moieties—Electron Transfer Capacities in Their Antitumoral Properties

DANEIDA LIZÁRRAGA,^{†,§} SONIA TOURIÑO,[#] FERNANDO J. REYES-ZURITA,[⊥]
 THEO M. DE KOK,[§] JOOST H. VAN DELFT,[§] LOU M. MAAS,[§] JACCO J. BRIEDÉ,[§]
 JOSEP J. CENTELLES,[†] JOSEP L. TORRES,[#] AND MARTA CASCANTE^{*,†,#}

Department of Biochemistry and Molecular Biology, unit associated with CSIC, Faculty of Biology, University of Barcelona, Biomedicine Institute of the University of Barcelona (IBUB), Diagonal 645, E-08028 Barcelona, Spain; Institute for Chemical and Environmental Research (IIQAB-CSIC), Jordi Girona 18-26, 08034 Barcelona, Spain; Biochemistry and Molecular Biology Department, Science Faculty, University of Granada, Campus Fuentenueva s/n, 18071 Granada, Spain; and Department of Health Risk Analysis and Toxicology, Maastricht University, P.O. Box 616, 6200 MD, Maastricht, The Netherlands

Witch hazel (*Hamamelis virginia*) extracts are used in traditional medicine. They are particularly rich in gallate esters included in proanthocyanidins, hydrolyzable tannins (galloylated sugars), and methyl gallate. This study examines the response of human colon cancer cells to treatment with fractions obtained from a witch hazel polyphenolic extract. The results are compared with those obtained previously with homologous fractions from grape (less galloylated) and pine (nongalloylated). Witch hazel fractions were the most efficient in inhibiting cell proliferation in HT29 and HCT116 human colon cancer cell lines, which clearly shows that the more galloylated the fractions, the more effective they were at inhibiting proliferation of colon cancer cells. Witch hazel fractions were, in addition, more potent in arresting the cell cycle at the S phase and inducing apoptosis; they also induced a significant percentage of necrosis. Interestingly, the apoptosis and cell cycle arrest effects induced were proportional to their galloylation. Moreover, witch hazel fractions with a high degree of galloylation were also the most effective as scavengers of both hydroxyl and superoxide radicals and in protecting against DNA damage triggered by the hydroxyl radical system. These findings provide a better understanding of the structure–bioactivity relationships of polyphenolics, which should be of assistance in choosing an appropriate source and preparing a rational design for formulations of plant polyphenols in nutritional supplements.

KEYWORDS: Antitumoral; DNA protection; gallate; scavenger; colon cancer; apoptosis; cell cycle

INTRODUCTION

Several phytochemicals (e.g., polyphenols) found in plants exert antioxidant and anticancer activities, including cell cycle arrest and induction of apoptosis in cancer cells (1, 2). Interest in plants as a source of bioactive compounds such as (–)-epigallocatechin-3-gallate (EGCG), (–)-epigallocatechin (EGC), (–)-epicatechin (EC), and (+)-catechin (C) has recently increased. Some of these polyphenols can be found in green tea

(*Camellia sinensis*), grape (*Vitis vinifera*), pine (*Pinus pinaster*), and witch hazel (*Hamamelis virginiana*) (3–6).

Plant polyphenols are natural antioxidants, and most of their pharmacological properties are understood to be based on their antioxidant capacity (7). This capacity is also generally considered to be linked to the scavenging of endogenously generated oxygen radicals or exogenous radicals produced by radiation or exposure to certain xenobiotics (8). A particularly valuable effect attributed to polyphenolics is their capacity to prevent oxidative DNA damage.

It has been suggested that EGCG, which is a galloylated compound and the major biologically active component of green tea, is associated with reduced risk of cancer through its pro-oxidant property (9). This anticancer effect has been linked to inhibition of cell growth, deregulation of cell cycle, and

* Author to whom correspondence should be addressed (telephone 0034934021593; fax 0034934021219; e-mail martacascante@ub.edu).

[†] University of Barcelona.

[§] Maastricht University.

[#] Institute for Chemical and Environmental Research (IIQAB-CSIC).

[⊥] University of Granada.

Table 1. Polyphenolic Composition of Witch Hazel, Grape, and Pine Extracts and Growth Inhibition Potency on HT29 and HCT116 Cells

plant source	fraction	% CT ^a	mDP ^b	% HT ^c	% G ^b	HT29 IC ₅₀ ^d (μg/mL)	HCT116 IC ₅₀ ^d (μg/mL)
witch hazel	VIIIH	4	1.1	96	97	35 ± 2	22 ± 2
	IVH	63	1.6	37	52	21 ± 2	36 ± 2
	VH	79	1	21	16	25 ± 2	27 ± 3
grape	VIIIG	>99	3.4	0	34	64 ± 4a	73 ± 4
	IVG	>99	2.7	0	25	59 ± 3a	82 ± 5
	VG	>99	1	0	0	119 ± 6a	122 ± 5
pine	VIIIP	>99	3	0	0	108 ± 5a	128 ± 6
	IVP	>99	2.9	0	0	106 ± 5a	128 ± 4
	VP	>99	1	0	0	422 ± 4a	447 ± 4

^a CT, condensed tannins: monomeric catechins and proanthocyanidins; molar percentage. ^b mDP (mean degree of polymerization) refers only to condensed tannins. % G (percentage of galloylation) adds up the contributions of both condensed and hydrolyzable tannins. mDP and %G from refs 4–6. ^c HT, hydrolyzable tannins (hamamelitannin, gallic acid, methyl gallate and pentagalloylglucose); molar percentage estimated by HPLC and standards. ^d IC₅₀ of grape and pine in HT29 from ref 14.

apoptosis induction (10–12). Moreover, other related compounds such as epicatechin, *trans*-resveratrol, and gallic acids have been described as antioxidant protectors in intestinal model systems (13). The influence of the polyphenolic structure on antioxidant activity, protective capacity, and, particularly, the mechanism of action remains open to debate, and further studies are required. It has been observed that polymerization and galloylation may render polyphenolics more or less reactive and bioavailable (14, 15).

It is usually argued that the extent of the potency of polyphenols *in vivo* is dependent on their metabolization and therefore their absorption (16). Some but not all polyphenols can be extensively degraded, metabolized, and absorbed through the gastrointestinal tract by several chemical reactions, but their final uptake is sometimes incomplete and their plasma and body levels are low (16). Indeed, there are several studies that demonstrate the presence of intact polyphenols in the gastrointestinal tract and suggest their importance as antioxidants, producing health-promoting activities in the colon (17, 18). The gallate esters are more stable than the simple catechins upon metabolization (19) and may be more bioavailable in the colon. Gallates have been reported to inhibit cell growth, trigger cell cycle arrest in tumor cell lines, and induce apoptosis (20). These chemical properties may be useful indicators for evaluating the potential of polyphenolic fractions for colon cancer prevention or treatment and the degree of polymerization related to the bioavailability in the colon.

For the present study we evaluated the inhibition of cell growth by witch hazel fractions on colorectal adenocarcinoma HT29 cells and the effect of those fractions on the cell cycle and induction of apoptosis through FACS analysis. Furthermore, we analyzed the properties of witch hazel fractions as scavengers of hydroxyl and superoxide radicals by ESR. We also compared the results obtained for the highly galloylated fractions from witch hazel with those from grape and pine. All of the fractions from the three sources (witch hazel, grape, and pine) were extracted using the same chemical procedures but differ in terms of gallate ester content (high, medium, and nil, respectively) and polymerization. All of the fractions were evaluated as protective agents against DNA damage through the measurement of 8-oxo-dG by HPLC. The results may help to clarify the role played by polyphenols from different sources and the relationship between structure and inhibition of cell proliferation, scavenger capacity, and DNA protection processes.

EXPERIMENTAL PROCEDURES

Materials. Dubelcco's Modified Eagle's Medium (DMEM) and Dubelcco's phosphate buffer saline (PBS) were obtained from Sigma

Chemical Co (St. Louis, MO), antibiotics (10000 units/mL penicillin, 10000 μg/mL streptomycin) were from Gibco-BRL (Eggenstein, Germany), and fetal calf serum (FCS) was from Invitrogen (Carlsbad, CA). Trypsin EDTA solution C (0.05% trypsin–0.02% EDTA) was purchased from Biological Industries (Kibbutz Beit Haemet, Israel). 3-[4,5-Dimethylthiazol-2-yl]-2,5-diphenyltetrazolium bromide (MTT), dimethyl sulfoxide (DMSO), propidium iodide (PI), and Igepal CA-630 were obtained from Sigma Chemical Co. NADH disodium salt (grade I) was supplied by Boehringer (Mannheim, Germany). RNase and agarose MP were obtained from Roche Diagnostics (Mannheim, Germany). Iron(II) sulfate heptahydrated was obtained from Merck (Darmstadt, Germany), α,α,α-Tris(hydroxymethyl)aminomethane was from Aldrich-Chemie (Steinheim, Germany) and moviol from Calbiochem (La Jolla, CA). Annexin V/FITC kit was obtained from Bender System (Vienna, Austria). The Realpure DNA extraction kit, including proteinase K, was obtained from Durviz S.L (Paterna, Spain). Blue/Orange loading dye and 1 kb DNA ladder were purchased from Promega (Madison, WI). 5,5-Dimethyl-1-pyrroline *N*-oxide (DMPO), hydrogen peroxide, phenazine methosulfate (PMS), and Hoescht were obtained from Sigma. DMPO was further purified by charcoal treatment. Salmon sperm DNA 2'-deoxyguanosine (dG) was obtained from Sigma.

Fractions. The polyphenolic fractions were obtained previously in our laboratories (4–6) and contain mainly monomeric catechins and procyanidins (OWG and OWP from grape and pine, respectively), which are soluble in both ethyl acetate and water. OWH from witch hazel contains mixtures of monomeric catechins, proanthocyanidins (procyanidins + prodelphinidins), and gallotannins (hydrolyzable tannins). The fractions derived from the extracts OWH, OWG, and OWP were generated by a combination of preparative reversed-phase high-performance liquid chromatography and semipreparative chromatography on Toyopearl TSK HW-40F (TosoHass, Tokyo, Japan), which separated the components by size and hydrophobicity. The phenolics were eluted from the latter column with MeOH (fractions VG and VP) and water/acetone 1:1 (fractions VIIIH, IVH, VH, VIIIG, IVG, VG, VIIIP, IVP, and V), evaporated almost to dryness, redissolved in Milli-Q water, and freeze-dried. The third to sixth columns in **Table 1** show the average chemical compositions of the fractions. Witch hazel fractions contain mainly small proanthocyanidins (monomers and dimers) so their mDPs are around 1 or 2. The composition of the fractions was estimated as previously described (4–6). Condensed tannins represented in **Figure 1** (monomeric catechins and proanthocyanidins) were estimated by thioacidolytic depolymerization and HPLC analysis of the cleaved units, and hydrolyzable tannins represented in **Figure 2** (HT, hamamelitannin, gallic acid, methyl gallate, and pentagalloylglucose) were determined directly from the fractions by HPLC and standards.

Cell Culture. Human colorectal adenocarcinoma HT29 cells (ATCC HTB-38) and HCT116 cells (ATCC CCL-247) were used in all experiments. HT29 and HCT116 cells were maintained in monolayer culture in an incubator with 95% humidity and 5% CO₂ at 37 °C. HT29

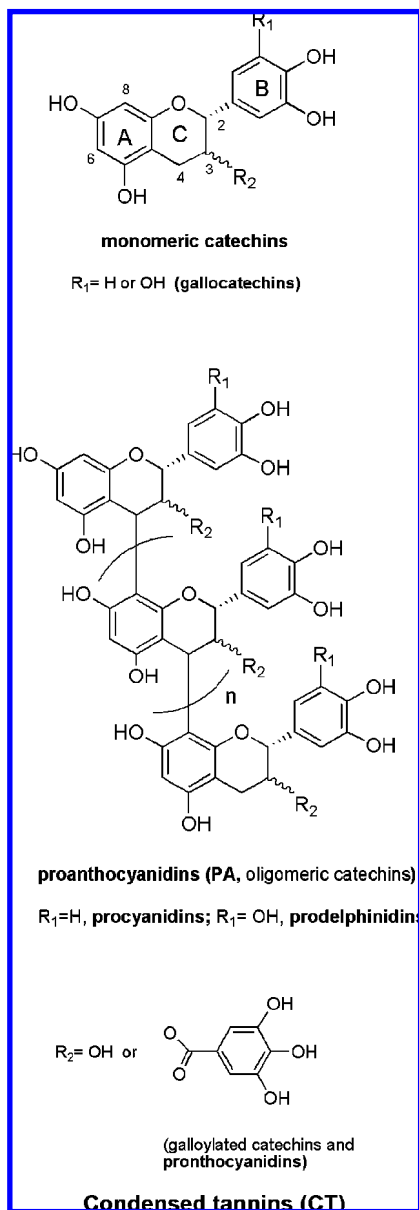


Figure 1. Structures of condensed tannins in *H. virginiana* bark extract.

and HCT116 cells were passaged at preconfluent densities using trypsin–EDTA solution C. Cells were cultured and passaged in DMEM supplemented with 10% heat-inactivated fetal calf serum and 0.1% streptomycin/penicillin.

Cell Growth Inhibition. HT29 and HCT116 were seeded at densities of 3×10^3 and 1.7×10^3 cells/well, respectively, in 96-well flat-bottom plates. After 24 h of incubation at 37 °C, the polyphenolic fractions were added to the cells at different concentrations from 5 to 2300 μM in fresh medium. The culture was incubated for 72 h, after which the medium was removed and 50 μL of MTT (5 mg/mL in PBS) with 50 μL of fresh medium was added to each well and incubated for 1 h. The blue MTT formazan precipitated was dissolved in 100 μL of DMSO, and the absorbance values at 550 nm were measured on an ELISA plate reader (Tecan Sunrise MR20-301, TECAN, Salzburg, Austria). Absorbance was proportional to the number of living cells. The growth inhibition concentrations that caused 50% (IC_{50}) and 80% (IC_{80}) cell growth inhibition were calculated using Graft 3.0 software. The assay was performed using a variation of the MTT assay described by Mosmann (21).

Cell Cycle Analysis. The assay was carried out using flow cytometry with a fluorescence-activated cell sorter (FACS). HT29 cells were plated in 6-well flat-bottom plates at a density of 87.3×10^3 cells/well. The number of cells was determined by cells/area well, as used in the cell

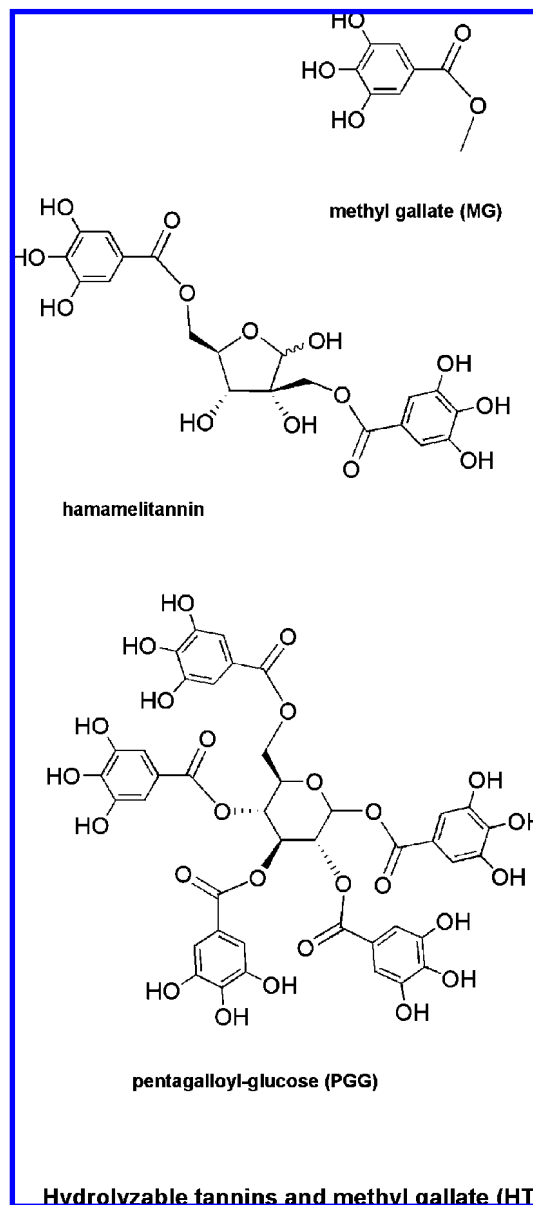


Figure 2. Structures of hydrolyzable tannins and methyl gallate in *H. virginiana* bark extract.

growth inhibition assay. The culture was incubated for 72 h in the absence or presence of the polyphenolic fractions at their respective IC_{50} values. Cells were then trypsinized, pelleted by centrifugation, and stained in Tris-buffered saline (TBS) containing 50 $\mu\text{g/mL}$ PI, 10 $\mu\text{g/mL}$ RNase free of DNase, and 0.1% Igepal CA-630 in the dark for 1 h at 4 °C. Cell cycle analysis was performed by FACS (Epics XL flow cytometer, Coulter Corp., Hialeah, FL) at 488 nm (22).

Apoptosis Analysis by FAC. Annexin V-FITC and propidium iodide staining were measured by FACS. Cells were seeded, treated, and collected as described in the previous section. Following centrifugation, cells were washed in binding buffer (10 mM HEPES, pH 7.4, 140 mM sodium chloride, 2.5 mM calcium chloride) and resuspended in the same buffer. Annexin V-FITC was added using the Annexin V-FITC kit. Following 30 min of incubation at room temperature and in the dark, propidium iodide (PI) was added 1 min before the FACS analysis at 20 $\mu\text{g/mL}$.

HPLC-ECD for Measuring 8-Oxo-dG. HPLC-ECD of 8-oxo-dG was based on a method described previously (23). Salmon DNA (1 mg/mL) was incubated as blank with Milli-Q water. The positive control of the experiment was performed using salmon DNA (1 mg/mL) incubated with Milli-Q water, 1 μM FeSO_4 , and 250 μM H_2O_2 , generating the hydroxyl radical system that induced the DNA lesion (8-oxo-dG), as a marker of oxidative damage. To assay the protection

capacity of the fractions in the induction of 8-oxo-dG, the witch hazel, grape, and pine fractions (VIIIH, IVH, VH, VIII G, IVG, VG, VIII P, IVP, and VP) were preincubated at 10, 25, 50, and 100 μ M. In all samples the incubation time was 10 min at room temperature, and then the hydroxyl radical systems were generated to simulate the oxidative stress exposure; samples were incubated for 30 min at 37 °C, and the reaction was stopped with a $1/30$ volume of 0.5 M NaAc. After that, DNA was digested into deoxyribonucleosides by treatment with nuclease P1 (0.02 unit/mL) and alkaline phosphatase (0.014 unit/mL) as was previously described (23). To minimize the possible induction of 8-oxo-dG during DNA handling, 10 mM 2,2,6,6-tetramethylpiperidine-1-oxide (TEMPO) was added to all solutions. The digest was then injected into a Gynkotec 480 isocratic pump (Gynkotec, Bremen, Germany) coupled with a Midas injector (Spark Holland, Hendrik Ido Ambacht, The Netherlands) and connected to a Supelcosil LC-18S column (250 \times 4.6 mm) (Supelco Park, Bellefonte, PA) and a Decade electrochemical detector (Antec, Leiden, The Netherlands). The mobile phase consisted of 10% aqueous methanol containing 94 mM KH_2PO_4 , 13 mM K_2HPO_4 , 26 mM NaCl, and 0.5 mM EDTA. Elution was performed at a flow rate of 1.0 mL/min with a lower detection limit of 40 fmol absolute for 8-oxo-dG or 1.5 residues/106 2'-deoxyguanosine (dG). 8-Oxo-dG was detected at a potential of 850 mV, and dG was simultaneously monitored at 260 nm. Results are expressed as percentages of the ratios of 8-oxo-dG to dG, relative to control ratios.

Electron Spin Resonance Spectroscopy. ESR measurements were performed at concentrations that caused 50% cell growth inhibition (IC_{50}). Fifty micromolar witch hazel fractions (VIIIH, IVH, and VH) were then compared with grape and pine fractions (VIII G, IVG, VG, VIII P, IVP, and VP). The molar concentrations of the fractions were calculated using the mean molecular masses estimated from the fraction compositions in **Table 1**. The mean molecular masses of the condensed tannins were estimated by thiolysis with cysteamine, as described in ref 24. $\cdot\text{OH}$ and $\text{O}_2^{\cdot-}$ formation was detected by ESR spectroscopy using DMPO (100 mM) as a spin trap. ESR spectra were recorded at room temperature in glass capillaries (100 μ L, Brand AG Wertheim, Germany) on a Bruker EMX 1273 spectrometer equipped with an ER 4119HS high-sensitivity cavity and 12 kW power supply operating at X-band frequencies. The modulation frequency of the spectrometer was 100 kHz. Instrumental conditions for the recorded spectra were as follows: magnetic field, 3490 G; scan range, 60 G; modulation amplitude, 1 G; receiver gain, 1×10^5 ; microwave frequency, 9.85 GHz; power, 50 mW; time constant, 40.96 ms; scan time, 20.97 s; number of scans, 25. Spectra were quantified by peak surface measurements using the WIN-EPR spectrum manipulation program (Bruker, Karlsruhe, Germany).

All incubations were done at room temperature; the hydroxyl radical generation system used 500 μ M FeSO_4 and 550 μ M H_2O_2 , and hydroxyl radicals generated in this system were trapped by DMPO, forming a spin adduct detected by the ESR spectrometer. The typical 1:2:2:1 ESR signal of $\text{DMPO}^{\cdot-}\text{OH}$ was observed. The superoxide radical generation system using 50 μ M of the reduced form of β -nicotinamide adenine dinucleotide (NADH) and 3.3 μ M phenazine methosulfate (PMS), and the superoxide radicals generated in this system were trapped by DMPO, forming a spin adduct detected by the ESR spectrometer. The typical ESR signal of $\text{DMPO}^{\cdot-}\text{OOH}/\text{DMPO}^{\cdot-}\text{OH}$ was observed. The $\cdot\text{OH}$ and $\text{O}_2^{\cdot-}$ scavenging activity was calculated on the basis of decreases in the $\text{DMPO}^{\cdot-}\text{OH}$ or $\text{DMPO}^{\cdot-}\text{OOH}/\text{DMPO}^{\cdot-}\text{OH}$ signals, respectively, in which the coupling constant for $\text{DMPO}^{\cdot-}\text{OH}$ was 14.9 G.

Data Presentation and Statistical Analysis. Assays were analyzed using Student's *t* test and were considered to be statistically significant at $* = P < 0.05$ and $** = P < 0.001$. Data shown were representative of three independent experiments, with the exception of ESR experiments that were performed in duplicate. ESR experiments were analyzed separately by radicals, two-way ANOVA was applied (day was a block factor; due to the nonsignificant effect of the day factor, we have reanalyzed with a one-way ANOVA), and finally multicomparison was done between compounds with respect to the control. ANOVA with Bonferroni and Scheffe posthoc tests was performed in ESR experiments.

RESULTS

Growth Inhibition Capacity. **Table 1** shows that witch hazel fractions containing highly galloylated tannins (VIIIH and IVH) dose-dependently reduced the proliferation of the carcinoma cell lines HT29 and HCT116 with IC_{50} average values of approximately 28 and 29 μ g/mL, respectively, whereas the IC_{50} of fraction VH containing around 16% of galloylation was effective in almost the same order (25 and 27 μ g/mL, respectively). It can also be observed that grape polyphenolic fractions VIII G and IVG obtained by the same extraction procedure as witch hazel fractions VIIIH and IVH have a percentage of galloylation of around 30% (approximately half or one-third that of the witch hazel fractions). On HT29 and HCT116, VIII G and IVG showed IC_{50} values of around 61 and 77 μ g/mL, respectively. Those concentrations were approximately double those of the homologous VIIIH and IVH witch hazel fractions required to exert the same cell growth inhibition on these cells. Moreover, for both cell lines IC_{50} of grape fraction VG was higher (119 and 122 μ g/mL, respectively). Pine fractions VIII P and IVP required a concentration almost 4 times higher than their homologues from witch hazel to exert the same effect in HT29 and HCT116 cells. In addition, the IC_{50} for fraction VP was almost 16 times higher than its counterpart from witch hazel. As pine fractions are not galloylated and grape fractions show almost half the galloylation of witch hazel fractions, we conclude that the more galloylated fractions are much more efficient than the less galloylated fractions in inhibiting colon carcinoma cell proliferation. This effect might also be modulated by the degree of polymerization of some components of the fractions (e.g., proanthocyanidins). Among monomers, those from witch hazel (galloylated) were more efficient than the less galloylated grape and pine counterparts. The results show that the more galloylated the fractions, the more effective they are at inhibiting proliferation of colon cells. These results confirm that galloylation enhances the antiproliferative capacity of polyphenolic fractions and indicate that natural polyphenolic fractions with a high degree of galloylation are more suitable as potential antitumoral agents than those containing no galloylation. This might be due to an enhanced electron transfer capacity (each gallate moiety provides three electrons) or a more specific activity attributed to the gallate group and not to other phenolic moieties.

Cell Cycle Analysis. The growth inhibition capacity of the fractions in HT29 and HCT116 from colon cancer followed almost the same pattern. We examined the effects of witch hazel fractions on the cell cycle at concentrations equal to their IC_{50} values in HT29 colon cancer cells. Cells were treated with each fraction for 72 h and then analyzed by FACS cytometer (**Figure 3**). The cell cycle distribution pattern induced after witch hazel polyphenolic treatments showed that, at IC_{50} , fraction VIIIH induced a significant decrease in G1 phase with respect to the control. In addition, the three fractions induced significant increases in S phase; interestingly, this induction was proportional to their percentage of galloylation. In phase G2 a significant decrease was induced by VIIIH. The most galloylated fraction (VIIIH) was the one that induced more deregulation in all stages of cell cycle in HT29 cells.

Apoptosis Induction. HT29 cell incubations with witch hazel polyphenolic fractions were performed at concentrations described under Materials and Methods. As shown in **Figure 4**, at IC_{50} concentrations, the witch hazel polyphenolic fractions VIIIH and IVH induced significant percentages of early apoptosis in HT29 cells as measured by FACS analysis. In addition, the three fractions (VIIIH, IVH, and VH) induced significant

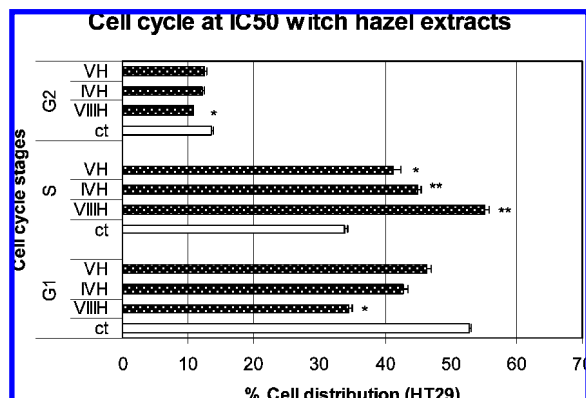


Figure 3. Cell cycle analysis of HT29 cells treated with witch hazel polyphenolic fractions at their respective grape IC₅₀ concentrations. Percentages of cells are shown in the different cell stages. Cell phases analyzed were G1, S, and G2 (% cells ± SEM; *, $p < 0.05$; **, $p < 0.001$). Experiments were performed in triplicate.

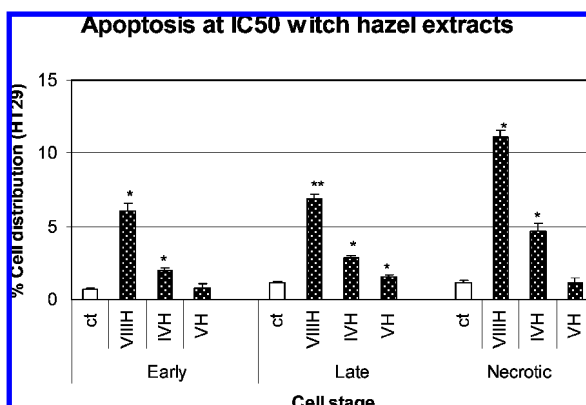


Figure 4. Apoptosis was induced in HT29 tumor cells. HT29 cells were treated with witch hazel polyphenolic fractions at their respective IC₅₀ concentrations. Percentages of cells are shown in different cell stages (on the x-axis) (% cells ± SEM; *, $p < 0.05$; **, $p < 0.001$). Experiments were performed in triplicate.

percentages in early/late apoptosis. Interestingly, this effect is proportional to their galloylation percentage. Fractions VIIIH and IVH also induced a significant percentage of necrosis, which could be due to a prooxidant effect at that concentration (25). This effect has also been observed for different polyphenolic compounds such as EGCG in HT29 and other tumoral cells (26, 27).

Protection Exerted by the Fractions against DNA Oxidative Damage. To evaluate the protective capacity of phenolics of different origins and compositions against DNA oxidative damage, salmon DNA incubation with fractions VIIIH, IVH, VH, VIIIH, IVG, VG, VIIIH, IVP, and VP was performed at 10, 25, 50, and 100 μM as described under Materials and Methods. Cells were preincubated with the fractions and thereafter exposed to a hydroxyl radical system. As shown in **Figure 5**, VIIIH, IVH, VIIIH, IVG, VIIIH, and IVP induced a dose-dependent protection against the hydroxyl radical, as given by the amount of the oxidative marker 7,8-dihydro-8-oxo-2'-deoxyguanosine (8-oxo-dg) (28) compared with the levels in 2'-deoxyguanosine (dG) of the cells. Low dose effects from fractions IVG, VIIIH, and IVP could be due to an interaction between polyphenols and traces of iron, which results in more radical-induced oxidative DNA damage in a hydroxyl radical generating system. A reasonable explanation for this phenomenon is that green tea polyphenols and flavonoids have metal-chelating properties combined with DNA-binding properties,

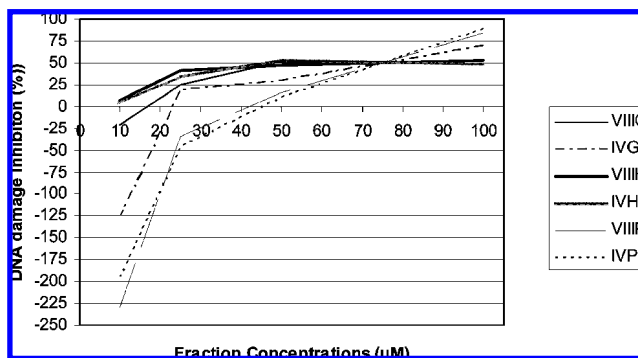


Figure 5. Witch hazel oligomeric fractions induced protection against DNA damage in the hydroxyl radical system. Percentages of protection produced at different fractions concentrations [concentrations (μM) shown on the x-axis] are shown (% protection ± SEM). Experiments were performed in triplicate.

thereby promoting hydroxyl radical production closely associated with the DNA (29). The dose-dependent decreases in the 8-oxo-dG to dG ratios indicate the efficiency of the fractions in protecting DNA from damage. The same DNA protection pattern has been observed for all of the fractions, with the witch hazel fractions providing the highest level of protection, followed by the grape fractions and finally by pine fractions (**Figure 5**). This property has recently been related to the antioxidant capacity exerted by several polyphenolic compounds. The monomeric fractions from witch hazel, grape, and pine (VH, VG, and VP) did not exert a protective effect (data not shown); this may be due to the concentration used in this assay. Moreover, to detect whether witch hazel fractions are also scavengers of the hydroxyl radical system, the scavenging capacity of the fractions was assayed by ESR.

Oxygen Radical Scavenging Activity As Detected by ESR Spectroscopy. The next set of experiments used ESR spectroscopy to test the radical scavenging capacity of the fractions against different biologically significant potentially harmful radicals. The results show that the VIIIH, IVH, VIIIH, IVG, VIIIH, and IVP, which were the most effective in antiproliferative assays on HT29 cells, were also the most efficient as hydroxyl radical and superoxide scavengers at 50 μM (**Figure 6A**). Fraction VIIIH was the most potent radical scavenger, followed by IVH, grape fractions VIIIH and IVG, and finally the pine fractions VIIIH and IVP. The same order of efficiency was also observed in the cell cycle arrest and induction of apoptosis observed in the present study and in our previous paper on grape and pine fractions (14). When fractions were tested at their respective IC₅₀ (**Figure 6B**), witch hazel phenolics were less effective as hydroxyl scavengers than grape and pine fractions. The same radical scavenging was observed on the superoxide anion radical system. This may be due to the low concentration used. At 50 μM , VH, VG, and VP (**Figure 6A**) were efficient hydroxyl scavengers; the fraction VH was the most effective, followed by VG fraction and VP fraction. These monomers did not show significant activity as superoxide anion radical scavengers. Again, the different order of efficacies as hydroxyl scavenger observed at their IC₅₀ (**Figure 6B**) for VH, VG, and VP may be attributed to the high concentrations used for monomers VG and VP (119 ± 6 and 422 ± 4 $\mu\text{g}/\text{mL}$, respectively) as opposed to the low concentration used for VH (25 $\mu\text{g}/\text{mL}$). In any case, VH from witch hazel was clearly more effective than VG and VP from grape and pine on the superoxide anion radical system.

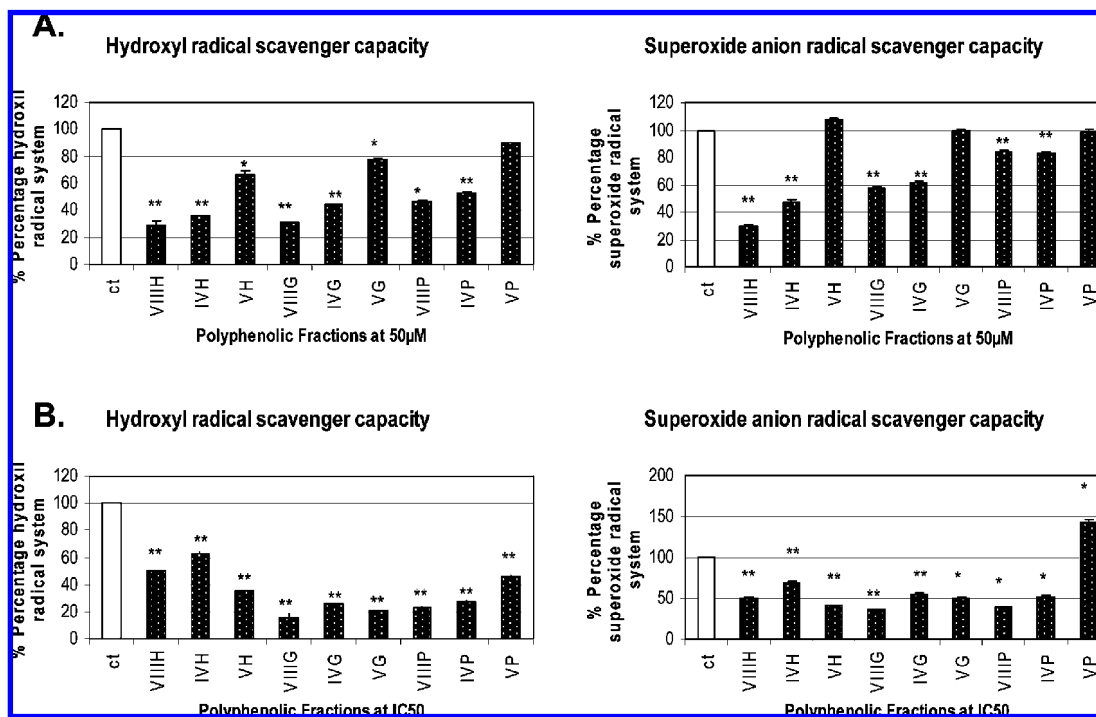


Figure 6. Scavenging activity of OH^\bullet and $\text{O}_2^{\bullet-}$ analyzed by ESR. Witch hazel, grape, and pine fractions were evaluated at (A) $50 \mu\text{M}$ and (B) IC_{50} concentration in HT29 cells in hydroxyl radical and superoxide anion radical generating systems, described under Experimental Procedures. Experiments were performed in duplicate (*, $p < 0.05$; **, $p < 0.001$). Data from grape and pine are from ref 18.

DISCUSSION

The present study shows that significant differences in the inhibition of cell growth in HT29 and HCT116 cells brought about by phenolics of different origins (fractions VIIIH, IVH, VH, VIIIIG, IVG, VG, VIIP, IVP, and VP) may be related to the structural properties of their components, mainly the percentage of galloylation and perhaps the degree of polymerization. Witch hazel fractions VIIIH, IVH, and VH were more effective than VIIIIG, IVG, VG, VIIP, IVP, and VP from grape and pine (Table 1). The same differences were observed in cell cycle deregulation and apoptosis induction on HT29 cells, the protective activity against DNA damage by oxidative stress, and the free radical scavenging capacities at the same concentration ($50 \mu\text{M}$). Galloylation appears to play an important role in the inhibition of cell growth. Even with monomers, galloylated VH was more potent than nongalloylated VG and VP. Fraction VIIIH was the most potent cell cycle deregulator, inducing significant changes in cell percentages of all the phases of the cell cycle. This fraction was also the most effective scavenger among those tested. Because the increases of cell percentages on the S phase of the cell cycle were proportional to their galloylation, this structural feature appears to be clearly significant for the explanation of the activity of phenolics, in accordance with our previous studies (14, 15). This highly galloylated fraction was also the most active apoptotic inducer and best free radical scavenger. The cell cycle arrest in the S phase observed for the three witch hazel fractions tested might be triggered by a change in the intracellular redox balance. Perturbations of the intracellular redox signals may block proliferation of tumor cells. It has been observed that cell membrane potentials change in response to H_2O_2 depending on the cell cycle phase. Intracellular ROS are particularly high in the S phase (30). Therefore, the cell cycle arrest induced by witch hazel fractions may be explained by their ROS scavenger capacity. Witch hazel fractions may block the cell cycle of HT29

cells in the S phase by scavenging ROS, with subsequent inhibition of DNA synthesis.

Because each gallate moiety provides three hydroxyl groups, galloylation clearly enhances the scavenger capacity of the fractions. Interestingly, galloylation also enhanced the induction of apoptosis and necrosis on HT29 cells. Fractions VIIIH and IVH induced both effects, whereas VH induced only some apoptosis. In this assay VIIIH also was the most active fraction, inducing around 13% of apoptosis and 11% of necrosis. The latter may be due to a pro-oxidant effect. This pro-oxidant effect of some polyphenolic fractions has been extensively discussed in the literature, where it has been described as a protective mechanism by up-regulation of genes implicated in the intracellular defense and biotransformation of xenobiotics such as enzymes of phases I and II (31).

There is a clear relationship between high galloylation percentages with low IC_{50} , cell cycle deregulation, apoptosis–necrosis induction, and scavenging capacity. Witch hazel fractions, which are heavily galloylated (Table 1), were more potent scavengers than grape and pine fractions in the two radical generation systems (hydroxyl and superoxide) at $50 \mu\text{M}$. This is due to the presence of pyrogallol moieties (three adjacent phenolic groups) in the form of gallates from both condensed and hydrolyzable tannins and gallo catechins (pyrogallol moieties in the condensed ring of proanthocyanidins). The main hydrolyzable tannins in the fractions are hamamelitannin (2',5'-di-*O*-galloyl hamamelose) and pentagalloyl glucose (6), included in Table 1 under HT. Moreover, witch hazel is a source of gallo catechins such as pyrogallol-containing epigallocatechin gallate (EGC), whereas grape and pine are mainly composed of epicatechin (EC) units. These structural features make witch hazel fractions effective electron donors (6). This could be behind the alleged pro-oxidant effect of some polyphenols. In fact, ROS may be formed by phenolics through one-electron reductions of molecular oxygen (O_2) to form the superoxide radical, which is primarily responsible for the cytotoxic effects

observed in aerobic organisms (32, 33). It has been observed that several pyrogallol-containing polyphenols, such as EGCG from green tea, exert their chemotherapeutic properties by modulating the cellular redox system on cells, including the production of reactive oxygen species, and influence glutathione metabolism and lipid peroxidation in different subcellular compartments (9). Moreover, it has been observed that antioxidant–prooxidant properties of ECGC are dose–response dependent (34). The redox states of polyphenolic flavonoids appear to influence their ability to induce oxidative molecular damage or antioxidant protective action (35). Nowadays, many natural polyphenolic extracts are commercialized, so it is crucial to increase knowledge of the polyphenolic structures within the extracts, the relationship with their putative antioxidant protective activity, and their mechanisms of action. The results presented here should be useful for a better understanding of structure–bioactivity relationships of polyphenolics, which should be of assistance in choosing an adequate source and a rational design for formulations of plant polyphenols in nutritional supplements and as chemotherapy in cancer.

LITERATURE CITED

- Seeram, N. P.; Adams, L. S.; Zhang, Y.; Lee, R.; Sand, D.; Scheuller, H. S.; Heber, D. Blackberry, black raspberry, blueberry, cranberry, red raspberry, and strawberry extracts inhibit growth and stimulate apoptosis of human cancer cells in vitro. *J. Agric. Food Chem.* **2006**, *54*, 9329–9339.
- Lee, S. Y.; Munerol, B.; Pollard, S.; Youdim, K. A.; Pannala, A. S.; Kuhnle, G. G.; Debnam, E. S.; Rice-Evans, C.; Spencer, J. P. The reaction of flavanols with nitrous acid protects against *N*-nitrosamine formation and leads to the formation of nitroso derivatives which inhibit cancer cell growth. *Free Radical Biol. Med.* **2006**, *40*, 323–334.
- Reto, M.; Figueira, M. E.; Filipe, H. M.; Almeida, C. M. Chemical composition of green tea (*Camellia sinensis*) infusions commercialized in Portugal. *Plant Foods Hum. Nutr.* **2007**, *62*, 139–144.
- Torres, J. L.; Varela, B.; García, M. T.; Carilla, J.; Matito, C.; Centelles, J. J.; Cascante, M.; Sort, X.; Bobet, R. Valorization of grape (*Vitis vinifera*) byproducts. Antioxidant and biological properties of polyphenolic fractions differing in procyanidin composition and flavonol content. *J. Agric. Food Chem.* **2002**, *50*, 7548–7555.
- Touriño, S.; Selga, A.; Jiménez, A.; Juliá, L.; Lozano, C.; Lizárraga, D.; Cascante, M.; Torres, J. L. Procyanidin fractions from pine (*Pinus pinaster*) bark: radical scavenging power in solution, antioxidant activity in emulsion, and antiproliferative effect in melanoma cells. *J. Agric. Food Chem.* **2005**, *53*, 4728–4735.
- Touriño, S.; Lizárraga, D.; Carreras, A.; Lorenzo, S.; Ugartondo, V.; Mitjans, M.; Vinardell, M. P.; Juliá, L.; Cascante, M.; Torres, J. L. Highly galloylated tannin fractions from witch hazel (*Hamamelis virginiana*) bark: electron transfer capacity, in vitro antioxidant activity and effects on skin related cells. *Chem. Res. Toxicol.* **2008**, *21*, 696–704.
- Adhami, V. M.; Mukhtar, H. Anti-oxidants from green tea and pomegranate for chemoprevention of prostate cancer. *Mol. Biotechnol.* **2007**, *37*, 52–57.
- Hofmann, T.; Liegibel, U.; Winterhalter, P.; Bub, A.; Rechkemmer, G.; Pool-Zobel, B. L. Intervention with polyphenol-rich fruit juices results in an elevation of glutathione *S*-transferase P1 (hGSTP1) protein expression in human leucocytes of healthy volunteers. *Mol. Nutr. Food Res.* **2006**, *50*, 1191–1200.
- Raza, H.; John, A. Green tea polyphenol epigallocatechin-3-gallate differentially modulates oxidative stress in PC12 cell compartments. *Toxicol. Appl. Pharmacol.* **2005**, *207*, 212–220.
- Yang, G. Y.; Liao, J.; Kim, K.; Yurkow, E. J.; Yang, C. S. Inhibition of growth and induction of apoptosis in human cancer cell lines by tea polyphenols. *Carcinogenesis* **1998**, *19*, 611–6.
- Jung, Y. D.; Kim, M. S.; Shin, B. A.; Chay, K. O.; Ahn, B. W.; Liu, W.; Bucana, C. D.; Gallick, G. E.; Ellis, L. M. EGCG, a major component of green tea, inhibits tumour growth by inhibiting VEGF induction in human colon carcinoma cells. *Br. J. Cancer* **2001**, *84*, 844–850.
- Shimizu, M.; Deguchi, A.; Lim, J. T.; Moriwaki, H.; Kopelovich, L.; Weinstein, I. B. (–)-Epigallocatechin gallate and polyphenon E inhibit growth and activation of the epidermal growth factor receptor and human epidermal growth factor receptor-2 signaling pathways in human colon cancer cells. *Clin. Cancer Res.* **2005**, *11*, 2735–2746.
- Kerem, Z.; Chetrit, D.; Shoseyov, O.; Regev-Shoshani, G. Protection of lipids from oxidation by epicatechin, *trans*-resveratrol, and gallic and caffeic acids in intestinal model systems. *J. Agric. Food Chem.* **2006**, *54*, 10288–10293.
- Lizárraga, D.; Lozano, C.; Briedé, J. J.; van Delft, J. H.; Touriño, S.; Centelles, J. J.; Torres, J. L.; Cascante, M. The importance of polymerization and galloylation for the antiproliferative properties of procyanidin-rich natural extracts. *FEBS J.* **2007**, *274*, 4802–4811.
- Lozano, C.; Juliá, L.; Jiménez, A.; Touriño, S.; Centelles, J. J.; Cascante, M.; Torres, J. L. Electron-transfer capacity of catechin derivatives and influence on the cell cycle and apoptosis in HT29 cells. *FEBS J.* **2006**, *273*, 2475–2486.
- Rice-Evans, C. Flavonoids and isoflavones: absorption, metabolism, and bioactivity. *Free Radical Biol. Med.* **2004**, *36*, 827–828.
- Jenner, A. M.; Rafter, J.; Halliwell, B. Human fecal water content of phenolics: the extent of colonic exposure to aromatic compounds. *Free Radical Biol. Med.* **2005**, *38*, 763–772.
- Halliwell, B.; Zhao, K.; Whiteman, M. The gastrointestinal tract: a major site of antioxidant action. *Free Radical Res.* **2000**, *33*, 819–830.
- Meselhy, M. R.; Nakamura, N.; Hattori, M. Biotransformation of (–)-epicatechin 3-*O*-gallate by human intestinal bacteria. *Chem. Pharm. Bull. (Tokyo)* **1997**, *45*, 888–893.
- Salucci, M.; Stivala, L. A.; Maiani, G.; Bugianesi, R.; Vannini, V. Flavonoids uptake and their effect on cell cycle of human colon adenocarcinoma cells (Caco2). *Br. J. Cancer* **2002**, *86*, 1645–1651.
- Mosmann, T. Rapid colorimetric assay for cellular growth and survival: application to proliferation and cytotoxicity assays. *J. Immunol. Methods* **1983**, *65*, 55–63.
- Lozano, C.; Torres, J. L.; Julia, L.; Jiménez, A.; Centelles, J. J.; Cascante, M. Effect of new antioxidant cysteinyl-flavanol conjugates on skin cancer cells. *FEBS Lett.* **2005**, *579*, 4219–4225.
- de Kok, T. M.; ten Vaarwerk, F.; Zwingman, I.; van Maanen, J. M.; Kleinjans, J. C. Peroxidation of linoleic, arachidonic and oleic acid in relation to the induction of oxidative DNA damage and cytogenetic effects. *Carcinogenesis* **1994**, *15*, 1399–1404.
- Selga, A.; Torres, J. L. Efficient preparation of catechin thio conjugates by one step extraction/depolymerization of pine (*Pinus pinaster*) bark procyanidins. *J. Agric. Food Chem.* **2005**, *53*, 7760–7765.
- Azam, S.; Hadi, N.; Khan, N. U.; Hadi, S. M. Prooxidant property of green tea polyphenols epicatechin and epigallocatechin-3-gallate: implications for anticancer properties. *Toxicol In Vitro* **2004**, *18*, 555–561.
- Hwang, J. T.; Ha, J.; Park, I. J.; Lee, S. K.; Baik, H. W.; Kim, Y. M.; Park, O. J. Apoptotic effect of EGCG in HT-29 colon cancer cells via AMPK signal pathway. *Cancer Lett.* **2007**, *247*, 115–121.
- Weisburg, J. H.; Weissman, D. B.; Sedaghat, T.; Babich, H. In vitro cytotoxicity of epigallocatechin gallate and tea extracts to cancerous and normal cells from the human oral cavity. *Basic Clin. Pharmacol. Toxicol.* **2004**, *95*, 191–200.

- (28) Zinov'eva, V. N.; Ostrovskii, O. V. Free radical oxidation of DNA and its biomarker oxidized guanosine(8-oxodG). *Vopr. Med. Khim.* **2002**, *48*, 419–431.
- (29) Leanderson, P.; Faresjo, A. O.; Tagesson, C. Green tea polyphenols inhibit oxidant-induced DNA strand breakage in cultured lung cells. *Free Radical Biol. Med.* **1997**, *23*, 235–242.
- (30) Gamaley, I. A.; Klyubin, I. V. Roles of reactive oxygen species: signaling and regulation of cellular functions. *Int. Rev. Cytol.* **1999**, *188*, 203–255.
- (31) Dhakshinamoorthy, S.; Long, D. J., 2nd; Jaiswal, A. K. Antioxidant regulation of genes encoding enzymes that detoxify xenobiotics and carcinogens. *Curr. Top. Cell Regul.* **2000**, *36*, 201–216.
- (32) Halliwell, B.; Gutteridge, J. M. Biologically relevant metal ion-dependent hydroxyl radical generation. An update. *FEBS Lett.* **1992**, *307*, 108–112.
- (33) Valko, M.; Leibfritz, D.; Moncol, J.; Cronin, M. T.; Mazur, M.; Telsler, J. Free radicals and antioxidants in normal physiological functions and human disease. *Int. J. Biochem. Cell Biol.* **2007**, *39*, 44–84.
- (34) Tian, B.; Sun, Z.; Xu, Z.; Hua, Y. Chemiluminescence analysis of the prooxidant and antioxidant effects of epigallocatechin-3-gallate. *Asia Pac. J. Clin. Nutr.* **2007**, *16*, 153–157.
- (35) Kim, B. H.; Cho, S. M.; Chang, Y. S.; Han, S. B.; Kim, Y. Effect of quercitrin gallate on zymosan A-induced peroxynitrite production in macrophages. *Arch. Pharm. Res.* **2007**, *30*, 733–738.

Received for review July 29, 2008. Revised manuscript received October 1, 2008. Accepted October 16, 2008. This work was supported by Grants PPQ2003-06602-C04-01 and -04, AGL2006-12210-C03-02/ALI, SAF2008-00164, doctoral fellowships to S.T. and D.L. from the Spanish Ministry of Education and Science, ISCIII-RTICC (RD06/0020/0046) from the Spanish government and the European Union FEDER funds and Generalitat de Catalunya (2005SGR00204; 2006ITT-10007).

JF802345X